Front. Optoelectron. China 2011, 4(3): 282–287
DOI 10.1007/s12200-011-0137-x

RESEARCH ARTICLE

Slow light in silicon microring resonators

Yingtao HU, Xi XIAO, Zhiyong LI, Yuntao LI, Yude YU, Jinzhong YU (✉)

State Key Laboratory on Integrated Optoelectronics, Institute of Semiconductors, Chinese Academy of Sciences, Beijing 100083, China

Abstract This paper experimentally investigated slow light effect in cascaded silicon-on-insulator (SOI) microring resonators. Double channel and single channel side-coupled integrated spaced sequence of resonators (SCISSOR) devices were fabricated with electron beam lithography and dry etching technology. The delay performances of the SCISSOR devices were demonstrated using non-return-to-zero (NRZ) and return-to-zero (RZ) signals at different bit rates. Group delays and bandwidths of cascaded microrings are significantly enhanced compared with single microring.

Keywords slow light, optical buffer, group delay, delay line, microring resonator

1 Introduction

Slow light, which means reducing light propagation velocity in media and structure, has become a rapidly growing field with a lot of potential applications and great scientific value. Especially, recent researches have indicated that slow light has good potential applications in variable optical delay lines or optical buffers of high-capacity communication networks [1,2], optical pulse synchronization [3], ultrafast all-optical information processing, quantum computing [4], nonlinear optical devices [5], true-time delay (TTD) in a phased-array antenna (PAA) [6,7], optical gyroscope and sensing [8,9], and miniaturization of many spectroscopy systems due to the availability of a variable delay line. The study of slow light also furthers our understanding of the fundamental physics of light, and nonlinear optical effects enhanced by slow light develop a new area for nonlinear optics.

There are many approaches to obtain slow light, such as material dispersion in atom vapors, optical fibers and semiconductor quantum wells; and waveguide dispersion in photonic crystals and resonant structures including microring resonators. Among most of these schemes, slow light based on microring resonators has attracted much attention for compact size and good integration on chip.

Silicon-on-insulator (SOI) is an attractive platform for monolithic integration of photonic devices due to its low cost and compatibility with standard complementary metal oxide semiconductor (CMOS) technology. Moreover, the high index contrast of the SOI material allows strong confined optical waveguides to reduce the size and power consumption of photonic devices.

In this paper, we first explored the operation principle of slow light in microring resonators using transfer matrix method, and the design of photonic delay lines based on passive cascaded microring were included. Then, we demonstrated our recent work on slow light based on cascaded SOI microring resonators. Both double channel and single channel side-coupled integrated spaced sequence of resonators (SCISSOR) [10] devices were fabricated with electron beam lithography and dry etching technology. Non-return-to-zero (NRZ) and return-to-zero (RZ) signals at different bit rates were used to demonstrate the delay performances of the SCISSOR devices.

2 Theory and design

The double channel SCISSOR consists of a series of add-drop microrings that are connected with each other by bus waveguides as shown in Fig. 1. Here, we used transfer matrix method [11] to analyze the transfer properties of the double channel SCISSOR, and similar results of the single channel SCISSOR can be obtained by setting all the coupling efficient at drop side to zero.

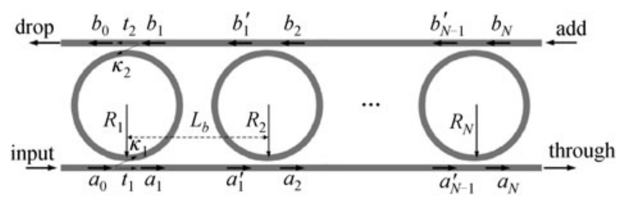

Fig. 1 Schematic diagram of double channel SCISSOR

Received March 24, 2011; accepted April 25, 2011

E-mail: jzyu@semi.ac.cn

For example, location optical fields (a_0, a_1 and b_0, b_1 as shown in Fig. 1) in the bus waveguides at the coupling areas of the first stage microring resonator are related by the coupling coefficient κ_1, κ_2 and transmission coefficient t_1, t_2 according to the following transfer matrix:

$$\begin{bmatrix} a_1 \\ b_1 \end{bmatrix} = \begin{bmatrix} t_{11} & t_{12} \\ t_{21} & t_{22} \end{bmatrix} \begin{bmatrix} a_0 \\ b_0 \end{bmatrix} \equiv T_1 \begin{bmatrix} a_0 \\ b_0 \end{bmatrix}, \qquad (1)$$

where

$$t_{11} = \frac{t_1 t_2 - a e^{\mathrm{i}\phi}}{t_2 - a t_1 e^{\mathrm{i}\phi}}, \qquad (2a)$$

$$t_{12} = -t_{21} = -\frac{a^{1/2}\kappa_1 \kappa_2 e^{\mathrm{i}\phi/2}}{t_2 - a t_1 e^{\mathrm{i}\phi}}, \qquad (2b)$$

$$t_{22} = \frac{1 - a t_1 t_2 e^{\mathrm{i}\phi}}{t_2 - a t_1 e^{\mathrm{i}\phi}}, \qquad (2c)$$

and a represents roundtrip amplitude attenuation in the ring, $\phi = n_r \cdot \frac{2\pi}{\lambda} \cdot 2\pi R$ is roundtrip phase shift in the ring. The light propagation in the two waveguides connecting each two adjacent rings can also be described using a transfer matrix:

$$\begin{bmatrix} a_1' \\ b_1' \end{bmatrix} = \begin{bmatrix} e^{-\eta + \mathrm{i}\phi_b} & 0 \\ 0 & e^{\eta - \mathrm{i}\phi_b} \end{bmatrix} \begin{bmatrix} a_1 \\ b_1 \end{bmatrix} \equiv T_{bus} \begin{bmatrix} a_1 \\ b_1 \end{bmatrix}, \qquad (3)$$

where η is field loss in the waveguides connecting each two adjacent rings, and $\phi_b = n_b \cdot \frac{2\pi}{\lambda} \cdot L_b$ is phase shift in the bus waveguide of length L_b. Therefore, the transfer matrix relation of the N-stage double channel SCISSOR can be obtained by cascading the transfer matrices of the elements,

$$\begin{bmatrix} a_N \\ b_N \end{bmatrix} = T_1 \cdot T_{bus} \cdot T_2 \cdot T_{bus} \cdot \ \cdots \ \cdot T_N \begin{bmatrix} a_0 \\ b_0 \end{bmatrix}. \qquad (4)$$

So power transmission and the phase shift of through port can be found from the total matrix as $T_{thr} = |a_N / a_0|^2$ and $\Phi_{thr} = \arg(a_N / a_0)$, respectively, and the group delay time can be derived as $\tau_{thr} = -\partial \Phi_{thr} / \partial \omega$. Similarly, results for the drop port can be obtained.

When multiple identical rings that have the same dimensions and the same coupling coefficients are cascaded, the resonances of each ring will locate at the same wavelengths and the group delay will be enhanced as well as the bandwidth. However, the insertion loss of cascaded structure is also increased. If a small resonance shift is introduced to each ring to make a spread for each individual resonance, the insertion loss will be reduced at the cost of a smaller total group delay. Meanwhile, the bandwidth will be much larger. It is a trade-off among the group delay, the bandwidth and the loss. Figure 2 shows the maximal group delay, the bandwidth and the insertion loss when different resonance spacings are introduced. In simulation, R = 10 μm, t_1 = 0.945, t_2 = 0.975, a = 0.99, $e^{-\eta}$ = 0.9985 and resolution of 0.001 nm. Obviously, the maximal group delay decreases monotonically with the resonance spacing. When the resonance spacing is too large, the maximal group delay falls to the level of the 1-stage ring. The bandwidth increases almost linearly with the increasing resonance spacing as shown in Fig. 2(a). If the resonance spacing is large enough, the insertion loss can be reduced to 1-stage ring's level as shown in Fig. 2(b). In summary, the resonance spacing should not be too small to get the enlarged bandwidth and the decreased insertion loss; meanwhile, the resonance spacing should not be too large so that the group delay can be significantly enhanced.

3 Devices and properties

The cascaded microring resonator devices are fabricated on a commercial single crystalline SOI wafer with a 340-nm-thick silicon slab on top of a 2 μm buried silica layer. The

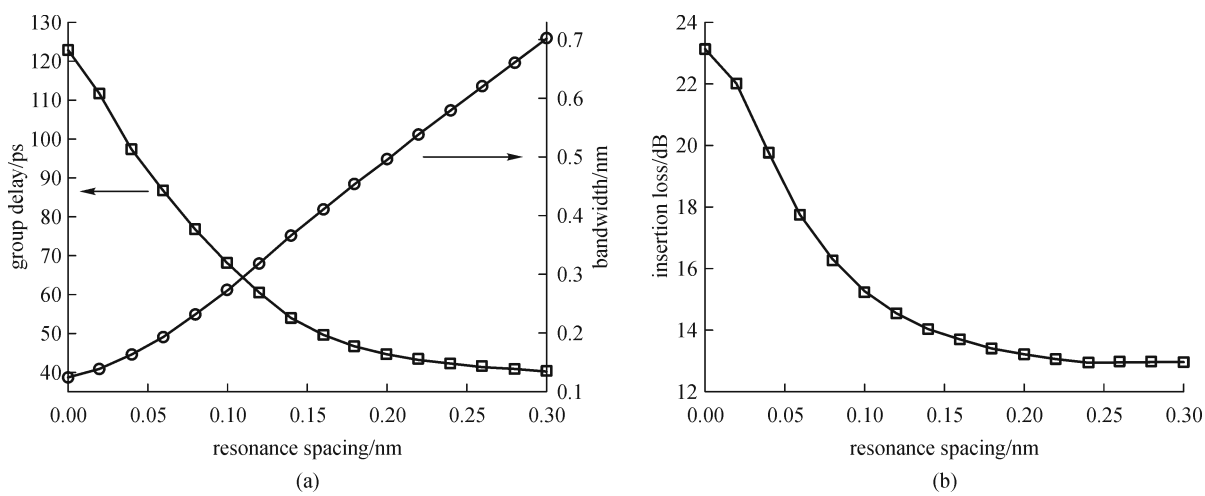

Fig. 2 Response curves of (a) maximal group delay, bandwidth and (b) insertion loss when different resonance spacings are introduced

cascaded microrings are formed by rib waveguide. For the convenience of fiber-to-device light coupling, grating couplers are integrated with the cascaded microrings. The microrings and the grating couplers are defined by one step of electron-beam-lithography (EBL). At first, a 170-nm-thick layer of polymethylmethacrylate (PMMA) is spun onto the SOI wafer and the microring structure together with gratings are patterned into the PMMA with Raith150 EBL system. After developing of the resist, the device pattern is transferred into the PMMA mask. Then, the pattern is etched into the silicon layer by inductively-coupled-plasma (ICP) etching processes. Controlling the etching processes the required depth is obtained and the rib waveguides is realized.

3.1 Double channel SCISSOR devices

A scanning electron microscopic (SEM) image of the fabricated cascaded microring structure is exhibited in Fig. 3(a). The radii of the microrings are 10 μm. The rib width of the bus waveguide and ring waveguide are 460 and 590 nm, respectively. The gaps between the bus waveguides and the ring waveguides are 180±5 nm at the through and 190±5 nm at the drop. The slab height is about 130 nm which corresponds to a 210 nm etch depth.

The measured through-port response spectra of the 1-stage and the 3-stage double channel SCISSOR devices are shown in Fig. 3(b). One can see that the spectral bandwidth is broadened from 0.09 nm (corresponding to 11 GHz) of the 1-stage device to 0.627 nm (corresponding to 78 GHz) of the 3-stage device. And the insertion loss is increased from 12.5 dB to 22.0 dB. From the spectral parameters of the 1-stage microring, the major optical parameters of the single ring resonator can be extracted: roundtrip attenuation factor, transmission and coupling coefficients are a = 0.99, t_1 = 0.9449, t_2 = 0.9749, κ_1 = 0.3274, κ_2 = 0.2226, respectively. These parameters completely describe the response of a resonator with a loaded Q of 3900, an intrinsic Q of 14000 and a group delay of 35.5 ps on resonance.

Non-return-to-zero (NRZ) pseudorandom bit sequence (PRBS) signals generated by a commercial $LiNbO_3$ modulator were used to experimentally demonstrate the delay performance. Figures 4(a)–4(d) demonstrate the measured results of the 3-stage double channel SCISSOR for input signal bit rates of 1 Gbps (Fig. 4(a)), 3 Gbps (Fig. 4(b)), 5 Gbps (Fig. 4(c)), and 12.5 Gbps (Fig. 4(d)), respectively. Blue curves are pulse waveforms when the signal wavelengths are off-resonant with the ring; and red curves are delayed pulse waveforms when the signal wavelengths are tuned on-resonant. The group delay time at different bit rates is almost 17 ps. Besides, the signal distortions of the delayed waveforms are negligible even at the highest measurement rate, which is also the limit of our equipments. This means that the bit rate does not reach the intrinsic bandwidth of the SCISSOR device. With the bandwidth of 78 GHz, the maximum allowable bit rate of 39 Gbps is expected [12].

3.2 Single channel SCISSOR devices

The SEM image of the 8-stage single channel SCISSOR device is shown in Fig. 5(a). The radii of the microrings are 6 μm. The rib width of the bus waveguide and ring waveguide are 460 and 590 nm, respectively. The slab height is about 130 nm which corresponds to a 210 nm etch depth.

The measured responses spectra of 1, 2, 4 and 8-stage cascaded microrings configured in single channel SCISSOR are shown in Fig. 5(b) in the same scale of both vertical axis and horizontal axis. One can see that the resonances are well matched in the 2-stage cascaded microrings, however, there are splits in the 4 and 8-stage cascaded microrings. Besides, the transmission resonances become much wider while increasing the cascaded stages. The spectra splitting and resonance broadening can be

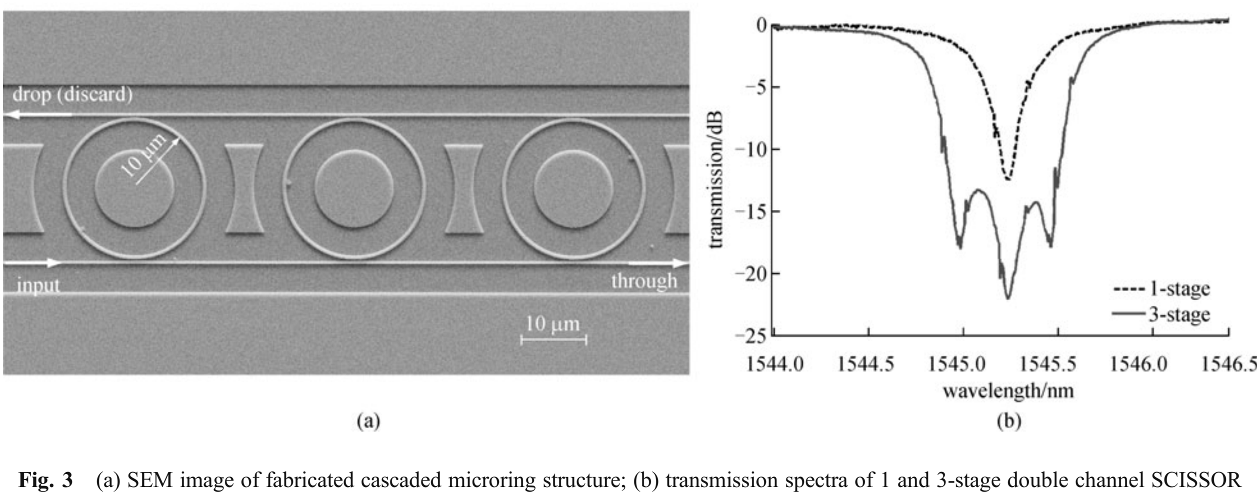

Fig. 3 (a) SEM image of fabricated cascaded microring structure; (b) transmission spectra of 1 and 3-stage double channel SCISSOR devices

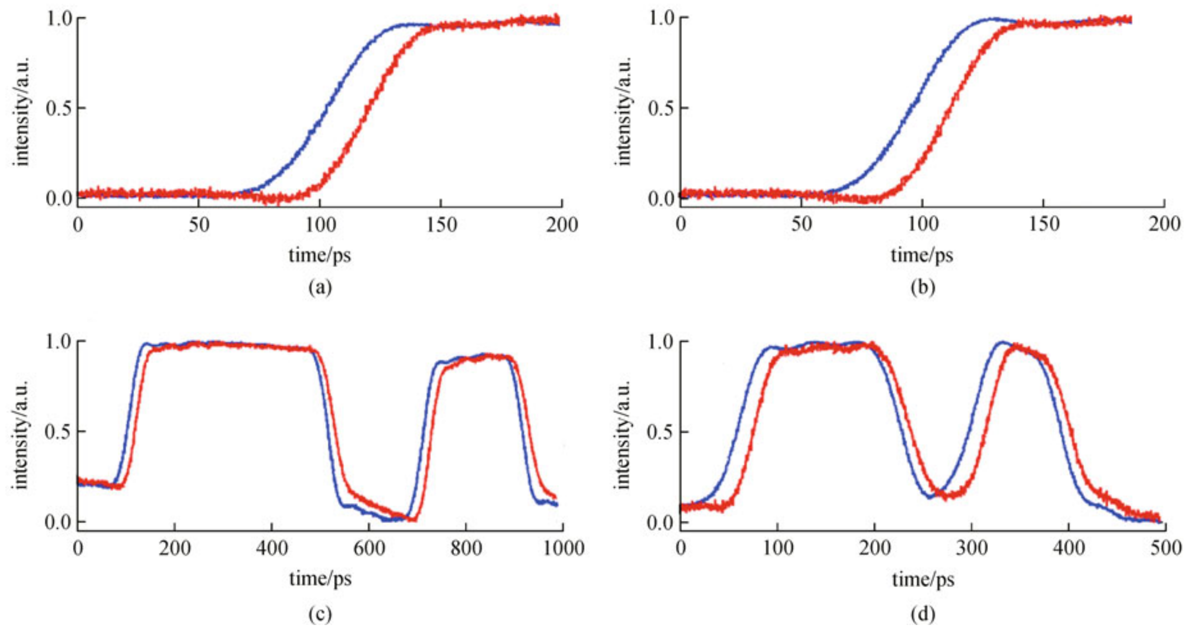

Fig. 4 Group delays of 3-stage double channel SCISSOR device at different bit rates. (a) 1 Gbps; (b) 3 Gbps; (c) 5 Gbps; (d) 12.5 Gbps

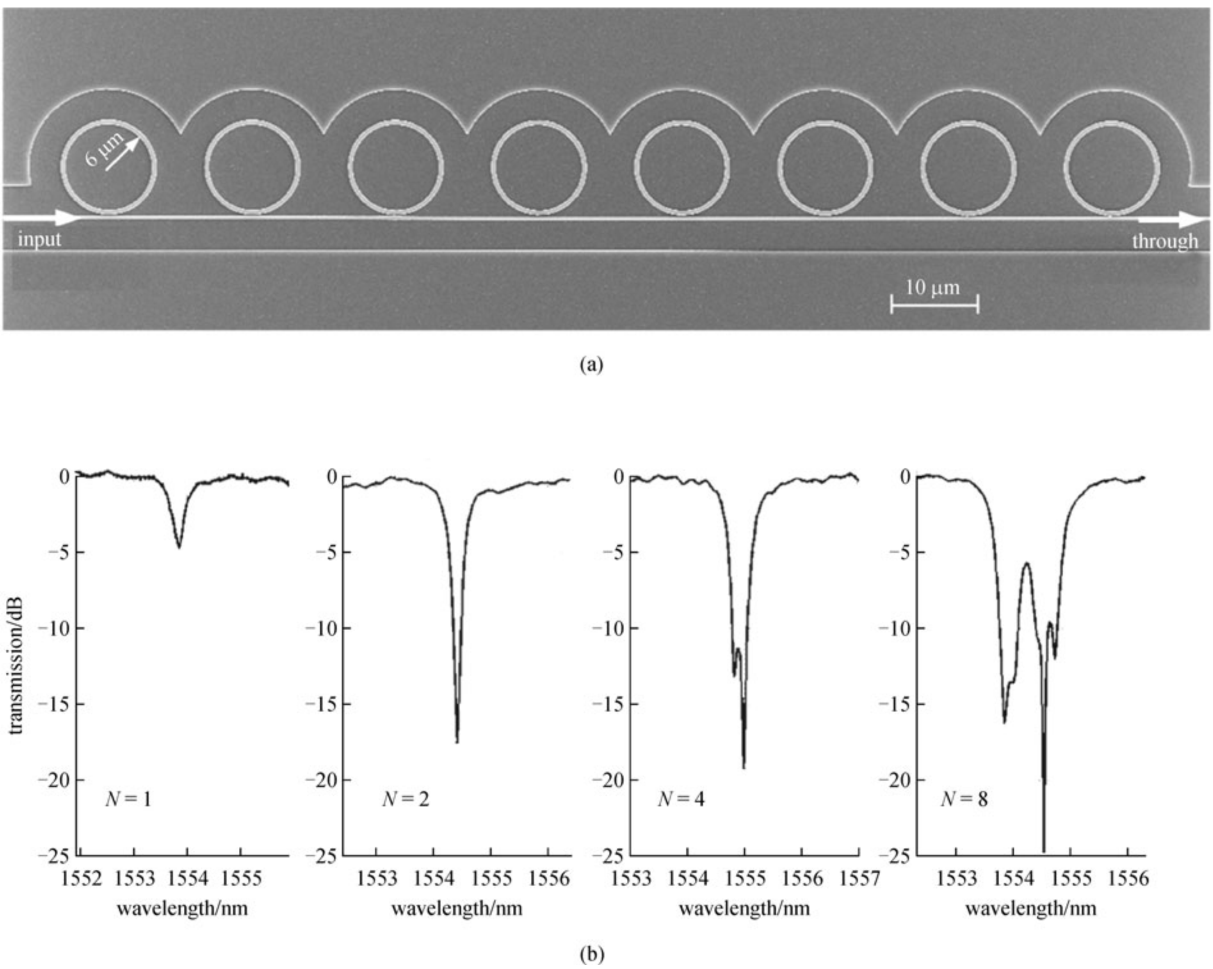

Fig. 5 (a) SEM image of 8-stage and (b) transmission spectra of 1, 2, 4 and 8-stage single channel SCISSOR devices

explained by a spread of individual resonances which can be caused by deviation of the coupling, the width of the waveguides, and the resonators' perimeters. The on-resonance insertion loss increases from 5 dB in the 1-stage to above 20 dB in the several-stage cascaded microrings. From the spectra parameters of 1-stage microring, we can extract the major optical parameters of single ring resonator: roundtrip attenuation factor (a), self-coupling (t) and cross-coupling (κ) coefficients and the results are $a = 0.9772$, $t = 0.9427$, $\kappa = 0.0573$, respectively. These parameters completely describe the response of a resonator with a loaded Q of 4560 and intrinsic Q of 26600 and group delay of 40 ps on resonance.

Return-to-zero (RZ) pulse train is used as a probe signal to experimentally demonstrate the pulse delay of the single channel SCISSOR devices. Figure 6 shows the time-domain measurements of a 1 Gbps (Fig. 6(a)) and 3 Gbps (Fig. 6(b)) sinusoidal signal of optical pulses in the RZ format, transmitted through the 1, 2, 4 and 8-stage single channel SCISSOR delay lines. Black solid curve refers to the pulse waveform while the signal wavelength is off-resonant with the ring, and the other four curves are the delayed pulse waveforms when the signal wavelength is tuned on-resonant within the 1, 2, 4 and 8-stage single channel SCISSOR, respectively. We can see that the pulse waveforms transmitted through 1 and 2-stage devices are delayed by ~ 25 ps, and the pulse through 4-stage devices is delayed by 38 ps, which value for 8-stage is 66 ps. It is clearly found that the group delays are enlarged while increase the cascaded stages, suggesting that the total delay of a cascaded microring structure is attributed to the summation of the delays of all the individual resonators. However, the 8-stage's delay is not exactly 8 times of the single-stage's delay. This can be explained that the delay variation of each ring and the resonant wavelength of the maximum delay of each ring is not exactly the same. We also use a 3 Gbps sinusoidal signal of optical pulses in an RZ format to test the group delays of our devices and the results are shown in Fig. 6(b). It can be observed that the group delay slightly decreased compare to the results of 1 Gbps. Besides, gentle distortion of the delayed pulse waveforms is observed. A possible explanation for the group delay decline and data degradation is the effect of large group delay dispersion (GDD) caused by the resonance splits. And lower optical power at a higher bit rate observed in the measurement may be another cause for the data degradation.

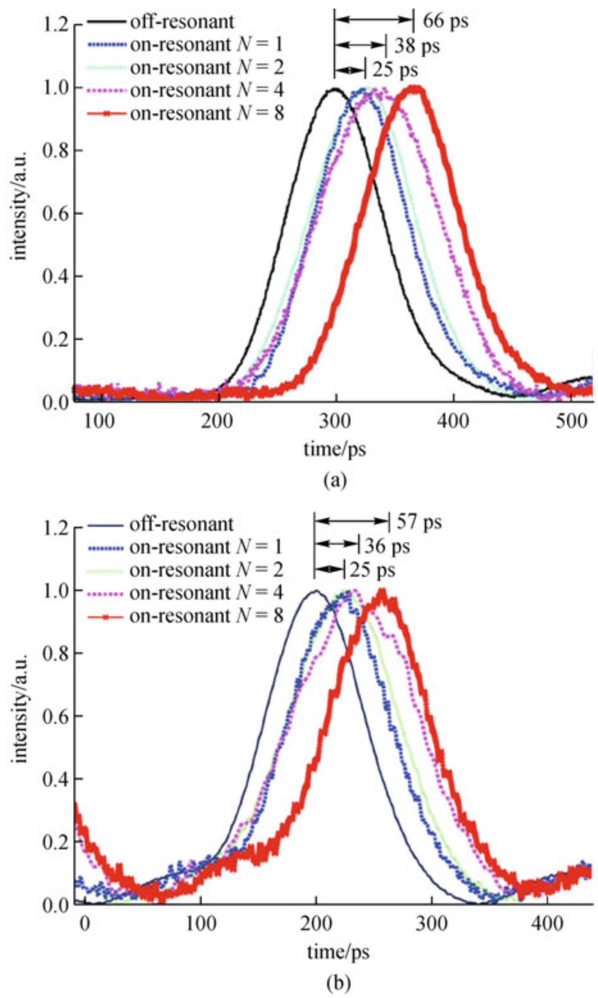

Fig. 6 Group delays of 1, 2, 4 and 8-stage single channel SCISSOR devices at (a) 1 Gbps and (b) 3 Gbps RZ signals

4 Conclusion

We have experimentally fabricated cascaded microrings based on SOI rib waveguides and examined their pulse delay performances. NRZ and RZ signals at different bit rates are used to demonstrate the delay performances of the SCISSOR devices. The SCISSOR devices are provided with both broader bandwidth and larger group delay than single microring. The maximum delay we have measured is 66 ps at 1-Gbps bit rate with our 8-stage single channel SCISSOR device, and the 3 dB spectral bandwidth suggested maximum allowable bit rate is large as 83 Gbps. We also suggest that much perfect resonance matching, which means negligible splits and low insertion loss of cascaded microrings, is the important point for optical delay line design.

Acknowledgements This work was supported by the National Basic Research Program of China (Nos. 2006CB302803 and 2011CB301701), the National Natural Science Foundation of China (Grant No. 60877036), State Key Laboratory of Advanced Optical Communication Systems and Networks, China (No. 2008SH02) and the Knowledge Innovation Program of Institute of Semiconductors, Chinese Academy of Sciences (No. ISCAS2008T10).

References

1. Boyd R W. Applications of slow-light in telecommunications and

optical switching. Presentation at Photonics West, 2006
2. Parra E, Lowell J R. Toward applications of slow light technology. Optics and Photonics News, 2007, 18(11): 40–45
3. Fisher M R, Chuang S L. Variable group delay and pulse reshaping of high bandwidth optical signals. IEEE Journal of Quantum Electronics, 2005, 41(6): 885–891
4. Fleischhauer M, Lukin M. Quantum memory for photons: dark-state polaritons. Physical Review A, 2002, 65(2): 022314
5. Harris S, Hau L. Nonlinear optics at low light levels. Physical Review Letters, 1999, 82(23): 4611–4614
6. Jemison W T, Yost T, Herczfeld P R. Acoustooptically controlled true time delays: experimental results. IEEE Microwave and Guided Wave Letters, 1996, 6(8): 283
7. Liu Z G, Zheng X P, Zhang H Y, Guo Y L, Zhou B K. X-band continuously variable true-time delay lines using air-guiding photonic bandgap fibers and a broadband light source. Optics Letters, 2006, 31(18): 2789–2791
8. Zhang Y D, Wang N, Tian H, Wang H, Qiu W, Wang J F, Yuan P. A high sensitivity optical gyroscope based on slow light in coupled-resonator-induced transparency. Physics Letters A, 2008, 372(36): 5848–5852
9. Wang N, Zhang Y D, Wang H, Tian H, Qiu W, Wang J F, Yuan P. Precise relative rotation sensing using slow light. Chinese Physics B, 2010, 19(1): 014216
10. Heebner J E, Chak P, Pereira S, Sipe J E, Boyd R W. Distributed and localized feedback in microresonator sequences for linear and nonlinear optics. Journal of the Optical Society of America B, Optical Physics, 2004, 21(10): 1818–1832
11. Heebner J E, Grover R, Ibrahim T. Optical Microresonators: Theory, Fabrication, and Applications. Springer Verlag, 2008
12. Xia F N, Sekaric L, Vlasov Y. Ultracompact optical buffers on a silicon chip. Nature Photonics, 2007, 1(1): 65–71